Appendix A

Reactions of Semivolatile Organics and Their Effects on Secondary Organic Aerosol Formation[*]

Reactions of Semivolatile Organics and Their Effects on Secondary Organic Aerosol Formation

JESSE H. KROLL,[†] ARTHUR W. H. CHAN, NGA L. NG, RICHARD C. FLAGAN, AND JOHN H. SEINFELD*

Departments of Environmental Science and Engineering and Chemical Engineering, California Institute of Technology, Pasadena, California 91125

Secondary organic aerosol (SOA) constitutes a significant fraction of total atmospheric particulate loading, but there is evidence that SOA yields based on laboratory studies may underestimate atmospheric SOA. Here we present chamber data on SOA growth from the photooxidation of aromatic hydrocarbons, finding that SOA yields are systematically lower when inorganic seed particles are not initially present. This indicates that concentrations of semivolatile oxidation products are influenced by processes beyond gas-particle partitioning, such as chemical reactions and/or loss to chamber walls. Predictions of a kinetic model in which semivolatile compounds may undergo reactions in both the gas and particle phases in addition to partitioning are qualitatively consistent with the observed seed effect, as well as with a number of other recently observed features of SOA formation chemistry. The behavior arises from a kinetic competition between uptake to the particle phase and reactive loss of the semivolatile product. It is shown that when hydrocarbons react in the absence of preexisting organic aerosol, such loss processes may lead to measured SOA yields lower than would occur under atmospheric conditions. These results underscore the need to conduct studies of SOA formation in the presence of atmospherically relevant aerosol loadings.

Introduction

Secondary organic aerosol (SOA), formed in the atmospheric oxidation of gas-phase organic compounds and subsequent gas-particle partitioning of lower-volatility reaction products, is known to be a major contributor to the total tropospheric particulate burden (*1*). As a result, our need for an accurate understanding of atmospheric aerosols and their effects requires that models of atmospheric chemistry include processes governing the formation and fate of SOA. Because the chemistry of SOA formation is so complex and uncertain, most descriptions of SOA formation (e.g., *2−4*) are semiempirical, constrained by environmental chamber studies of SOA formation and growth.

The primary framework for including SOA formation in atmospheric chemistry models, and relating the amount of aerosol generated in chambers with that in the troposphere, is the treatment of condensable species in SOA as semivolatile organics, present in appreciable amounts in both the gas and particle phases. Work by Pankow (*5*, *6*) and Odum et al. (*7*) demonstrated that SOA yield Y (defined as $\Delta M/\Delta HC$, the amount of aerosol formed per hydrocarbon reacted) can be expressed in terms of the gas-particle partitioning of a collection of i semivolatile species:

$$Y = \frac{\Delta M}{\Delta HC} = M \sum_i \frac{\alpha_i K_{p,i}}{1 + M K_{p,i}} \qquad (1)$$

in which α_i and $K_{p,i}$ are the stoichiometric coefficient and gas−particle partitioning coefficient of species i, respectively, and M is the mass concentration of absorbing (typically organic) aerosol present. Therefore SOA formation is a function of not only the amount and volatility of the semivolatile compounds, but also the aerosol mass into which they can partition. This non-stoichiometric nature of aerosol yields is a known feature of SOA formation, and aerosol growth data have been shown to be well-represented by eq 1 (typically as "yield curves", plots of Y vs M) (*7*, *8*). This expression is also used to describe SOA formation in the atmosphere: α's and K_p's for a given hydrocarbon are those determined in chamber studies, and M is the ambient atmospheric organic aerosol mass loading, typically 1−20 $\mu g/m^3$. However, recent work suggests that this semiempirical approach, in which SOA formation is estimated based on experimentally determined aerosol yields, generally predicts SOA levels that are substantially lower (often by an order of magnitude or more) than measured values (*2−4*). Such discrepancies suggest that the reaction conditions of environmental chambers may lead to less SOA growth than occurs in the atmosphere, though unidentified SOA precursors may also play a role.

In this work we examine a chemical system for which SOA yields are dependent on the timing of the onset of gas-particle partitioning. Specifically it is shown that in the photooxidation of aromatic compounds, aerosol growth begins sooner, and hence aerosol yields are higher, in the presence of seed particles. Such an effect indicates that processes governing the amount of SOA formed are more complex than the simple formation and condensation of semivolatile compounds. Additional reactions of semivolatile organics may occur in both the gas and particle phases, changing the concentration and/or volatility of the organics. We examine the kinetics and partitioning of a model semivolatile compound which may undergo reactions in the gas and particle phases, in order to better understand the effect of such reactions on SOA growth. It is also shown that in the absence of initial absorbing aerosol mass, SOA yields as measured in chambers may be significantly lower than those in the real atmosphere.

Experimental Section

SOA formation from the photooxidation of aromatic hydrocarbons was measured using experimental protocols described previously in detail (*9−11*). Briefly, ∼3 ppm H_2O_2 (the OH precursor) and the aromatic (71−72 ppb *m*-xylene or 87−91 ppb toluene, Aldrich) are added to a 28 m^3 Teflon chamber; for some experiments NO and/or ammonium sulfate seed are also added. For "NO_x" experiments, initial NO and NO_2 levels are 85 ± 4 ppb and 6 ± 4 ppb, respectively (otherwise NO_x levels are <1 ppb), and for "seeded" experiments, seed number concentrations are $21\,000 \pm 4000$ particles/cm^3 (otherwise concentrations are <5/cm^3). Reaction begins when the blacklights surrounding the chamber

* Corresponding author phone: (626) 395-4635; fax: (626) 796-2591; e-mail: seinfeld@caltech.edu.

† Current address: Aerodyne Research, Inc., 45 Manning Road, Billerica MA 01821.
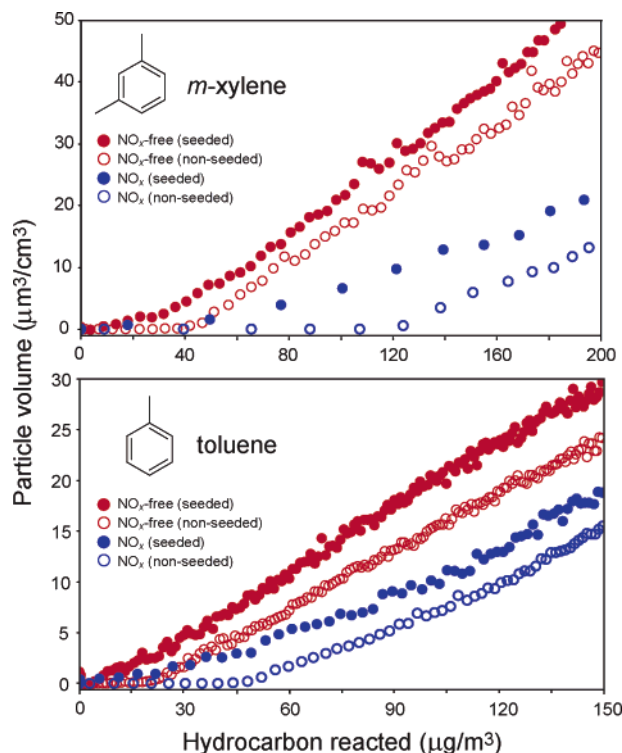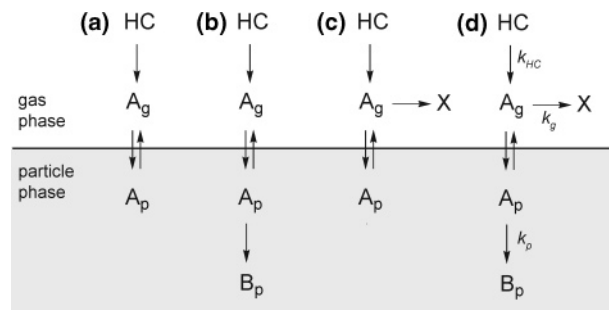
FIGURE 1. "Growth curves" for photooxidation of *m*-xylene and toluene. Each curve represents a single experiment; individual points are in 4 min increments. Color denotes NO$_x$ condition (red, NO$_x$-free; blue, ~90 ppb NO$_x$ initially present) and symbol denotes seed (filled circles, ammonium sulfate seed present; open circles, no seed present). In all nonseeded experiments there is a substantial induction period, leading to lower SOA yields.

FIGURE 2. Mechanisms for SOA formation from a single semivolatile species A: (a) simple gas−particle partitioning, the standard model for SOA growth; (b) gas−particle partitioning followed by irreversible reaction to form nonvolatile product B$_p$; (c) competition between gas−particle partitioning and irreversible loss of the gas-phase semivolatile compound; (d) both gas- and particle-phase reactions in addition to partitioning.

are turned on; hydrocarbon concentration is monitored by gas chromatography−flame ionization detection, and aerosol volume is monitored by a differential mobility analyzer. Particle volume is corrected for losses of particles to the walls (*10*). Temperature and relative humidity are the same in all experiments (initial values of 23−25 °C and 4−7%, respectively). A total of eight experiments, systematically varying aromatic hydrocarbon (toluene vs *m*-xylene), ammonium sulfate seed ("seeded" vs "nonseeded"), and NO$_x$ level ("NO$_x$" vs "NO$_x$-free"), were conducted.

Results and Discussion

Shown in Figure 1 is SOA growth from the four pairs of seeded/nonseeded experiments. Data are presented as "growth curves", plots of aerosol growth vs hydrocarbon reacted. As hydrocarbon measurements are made with much lower frequency than those of particle volume, the HC values shown are obtained by interpolation of GC measurements, fitting the data to a double-exponential decay (which reproduces measured hydrocarbon concentrations well, R^2 > 0.95). Only the growth near the beginning of the experiments (including the atmospherically relevant range of *M*) is shown; beyond this, the shapes of the curves do not change substantially, remaining slightly curved until all hydrocarbon is consumed ($\Delta HC = HC(0)$). Aerosol yields are generally higher than previously reported for aromatic photooxidation (*12*), likely a result of the lower NO$_x$ levels employed in this work (*13, 14*).

We focus on the systematic differences between aerosol growth in the seeded and nonseeded cases; the effects of the other parameters varied (such as NO$_x$ level) are beyond the scope of this work and are discussed elsewhere (*15*). The presence of seed is expected to have a negligible effect on hydrocarbon oxidation, and indeed the observed decays of

the hydrocarbon (from reaction with OH) are the same in seeded and nonseeded experiments. However, in all cases the aerosol growth exhibits a marked dependence on whether seed particles are present. In all seeded experiments, SOA growth is observed to begin essentially immediately, whereas in all nonseeded experiments, there is a substantial "induction period", a period of time during which the parent hydrocarbon reacts away but no aerosol is formed. The amount of hydrocarbon reacted during this period in the nonseeded cases ranges from 20 μg/m^3 (~5 ppb) for the toluene/NO$_x$-free experiment to 120 μg/m^3 (~27 ppb) for the *m*-xylene/NO$_x$ experiment. Once SOA growth begins, its rate is the same as in the seeded experiments, leading to roughly fixed differences in ΔM at a given value of ΔHC, and hence differences in SOA yields. Such differences persist throughout the experiments, but are most pronounced at lower (atmospherically relevant) aerosol loadings: for example, in the *m*-xylene/NO$_x$ experiments, at $M = 5$ μg/m^3 SOA yield in the seeded case is almost twice that of the nonseeded case (assuming densities are similar). We note that such a difference between yields in seeded and nonseeded experiments was not observed in an earlier study of high-NO$_x$ photooxidation of *m*-xylene from our laboratory (*16*); in that study there were few data at low (<25 μg/m^3) aerosol loadings, the condition at which this effect is most pronounced, as well as higher scatter in the yield results than we currently observe (*10*), and possibly differing chemistry due to higher NO$_x$ levels.

The observed effect of seed on SOA growth implies differences in effective gas-particle partitioning coefficients (*17*): partitioning into the particle phase is stronger in the seeded experiments than in the nonseeded ones. This difference cannot be explained by the simple model of SOA formation described in the Introduction (and shown in Figure 2a): the semivolatile species initially formed are the same regardless of the presence of seed, and the solid seed particles cannot promote absorptive partitioning. Instead, the distribution of reaction products must be affected by additional processes, leading to enhancements in lower-volatility compounds in the presence of seed particles, and/or decreases in their absence.

The former possibility is consistent with recent work suggesting that particle-phase reactions, forming high-MW, low-volatility products, are important processes in SOA formation. The formation of such compounds, including oligomers (*18−24*) and organosulfates (*25−27*), is accompanied by the depletion of the semivolatile reactants in the particle phase; the resulting shift in the gas-particle equilibrium leads to more SOA formation than would be inferred on the basis of physical partitioning alone (*14, 28*). Many

such products are thermally stable (e.g., *18, 24−27*), suggesting they are relatively long-lived, and canot quickly revert to reactants. While the reversiblity of SOA formation over long time scales is highly uncertain (experimental studies are largely lacking at present), the formation of high-MW species may be approximated as an irreversible step, so long as decomposition occurs on time scales longer than the time scales studied. Oxidation of aerosol components ("photochemical aging") is another mechanism by which lower-volatility compounds may be irreversibly formed. The irreversible formation of nonvolatile species in SOA suggests the reaction scheme shown in Figure 2b, in which the semivolatile species (A_p) reacts further in the condensed phase to form a purely particle-phase species (B_p). The promotion of such reactions by ammonium sulfate particles may account for the differences in SOA growth illustrated in Figure 1.

Alternately, such differences could result from reactions of semivolatile species forming products other than SOA. Such processes serve to lower the concentration of the gas-phase species, thereby reducing the amount that partitions into the aerosol phase. Shown in Figure 2c is such a mechanism, in which the gas-phase semivolatile organic (A_g) reacts to form X, a generic non-particle-phase product. This may be a volatile species present only in the gas phase, formed by bond-breaking oxidation or photolysis reactions; or it may represent organics lost to the chamber walls. Such losses of semivolatile species have received little study in terms of their role in SOA formation, but certainly occur in many cases. For example, it has been shown that photolysis of organic aerosol components forms relatively volatile organics (*29−31*), which lead to reductions in SOA mass. Similarly, glyoxal, formed in the oxidation of aromatics, is known to efficiently partition into the particle phase (*25, 32, 33*), but it is also known to react with OH, photolyze, and be taken up onto surfaces; all these processes are expected to compete with gas-particle partitioning and hence reduce SOA growth.

Thus additional reactions of semivolatile organics, such as those shown in Figure 2b and c, may qualitatively explain differences in SOA yields between seeded and nonseeded photooxidation experiments (Figure 1). However, neither scheme represents a reasonable mechanism by which all semivolatile compounds will react: in one case (Figure 2b) all the organic is incorporated into the gas phase, so growth does not depend on gas-particle partitioning, and in the other (Figure 2c), at long reaction times no SOA is formed at all. Instead, most SOA-forming reactions involve a spectrum of semivolatile products, which likely exhibit varying chemistries, including reactions in both phases. The generalized mechanism shown in Figure 2d, in which the semivolatile species A can react by both pathways in Figure 2b and c, serves as a useful model system for investigating the role of the reactions of semivolatile organics in SOA growth, and may even roughly approximate the behavior of a more complex mixture. In this scheme, SOA yields are dependent not only on the volatility of the product A, but also on the rates of these additional reactions. In the following sections, we illustrate the possible role of such chemistry on aerosol growth. The dependence of SOA growth on the presence of seed particles is predicted, due largely to the delayed onset of gas-particle partitioning in the nonseeded case.

Model Description. The mechanism shown in Figure 2d is considered for only a single semivolatile species; we emphasize this is not intended to be a detailed mechanism of SOA formation, but rather a model system for studying the role of additional chemical reactions on gas−particle partitioning. All steps in the mechanism are represented as unimolecular processes, with rate constants k_{HC}, k_g, and k_p for the reactions HC→A_g, A_g→X, and A_p→B_p, respectively. For simplicity, specific reaction conditions such as oxidant level are omitted, and all reactions are assumed to be irreversible over the time scale of the simulation; the effects of specific reaction conditions and reversible processes are beyond the scope of this work, but are worth further study. Gas−particle partitioning is treated as in Bowman et al. (*34*), with the net rate of uptake of a species by physical partitioning given by *J*, its flux to the particle surface:

$$J = \frac{N_p \, 2\pi \, D_p \, \lambda \, \bar{c} \, ([A_g] - [A_g]_{eq})}{1 + \frac{8 \, \lambda}{\alpha_c \, D_p}} \qquad (2)$$

in which N_p is the particle number density, D_p is the diameter of the particle, λ is the mean free path of air (65 nm), $\bar{c}$ is the mean molecular speed of the species, α_c is the accommodation coefficient, and $[A_g]$ and $[A_g]_{eq}$ are the mass concentrations of the bulk and near-surface (equilibrium) gas-phase species, respectively. $[A_g]_{eq}$ is calculated by absorptive partitioning (*5*):

$$[A_g]_{eq} = \frac{[A_p]}{K_p \, M} = \frac{[A_p]}{K_p \, ([A_p] + [B_p] + M(0))} \qquad (3)$$

in which $M(0)$ is mass concentration of preexisting organic aerosol. For simulations of reactions carried out in the absence of organic aerosol (i.e., chamber experiments), initial absorbing aerosol mass loading $M(0)$ is set to a very small but nonzero value (0.1 ng/m³). The kinetics of gas−particle partitioning (eq 2) require values for D_p and N_p; to simplify the modeling, three assumptions are made: (1) particle number concentration is fixed at 2×10^4/cm³, (2) the aerosol population is monodisperse, and (3) the organic aerosol has unit density. Relaxation of any of these assumptions is expected to have a minimal effect on model results.

For the simulations discussed here, the parent hydrocarbon reacts with rate $k_{HC} = 0.015$ min⁻¹, forming A with a stoichiometric yield of 0.2, reasonable values for an SOA-forming reaction. Rates of the reactions of species A are chosen to be comparable to hydrocarbon oxidation, with $k_p = k_{HC}$ and $k_g = 0.3 \, k_{HC}$; if the reactions were substantially slower, their effects would not be observed on the time scale of chamber experiments. The semivolatile compound A is assigned a K_p of 0.1 μg^{-1} m³ (for a saturation vapor pressure of 10 μg/m³), $\bar{c}$ of 200 m/s (corresponding to a MW of ~150 g/mol), and α_c of 0.02 (as determined for glyoxal (*34*)). For most simulations, only the initial conditions (*HC*(0), *M*(0), and seed volume) are varied.

Model Predictions. Figure 3a shows concentrations as a function of time after reaction initiation, for conditions typical of "seeded" chamber experiments: initial hydrocarbon concentration is relatively high (HC(0) = 91 μg/m³), and the preexisting aerosol seed is ammonium sulfate (20 μg/m³), with negligible initial organic mass (*M*(0) = 0.1 ng/m³).

Following reaction initiation, there is an induction period, a result of the absence of absorbing aerosol into which the semivolatile organic may partition. Thus the semivolatile species increases in concentration in the gas phase, during which time some fraction reacts away to form X. Only when A_g approaches its saturation vapor pressure does partitioning begin and SOA mass is formed. After ~12 h all the hydrocarbon is reacted away, A has fully reacted to form X or B_p, and aerosol formation is completed, with $\Delta M = 10$ μg/m³. Thus the SOA mass yield is 11% at an organic aerosol loading of 10 μg/m³.

SOA yields over a range of aerosol mass loadings are generally determined by varying the amount of hydrocarbon reacted, which leads to differences in *M*. Calculated yields over a range of *M*'s are presented in Figure 4 (curve a). The curve of yield vs *M* (over the atmospherically relevant range of *M*'s) has the qualitative shape of a typical "yield curve",
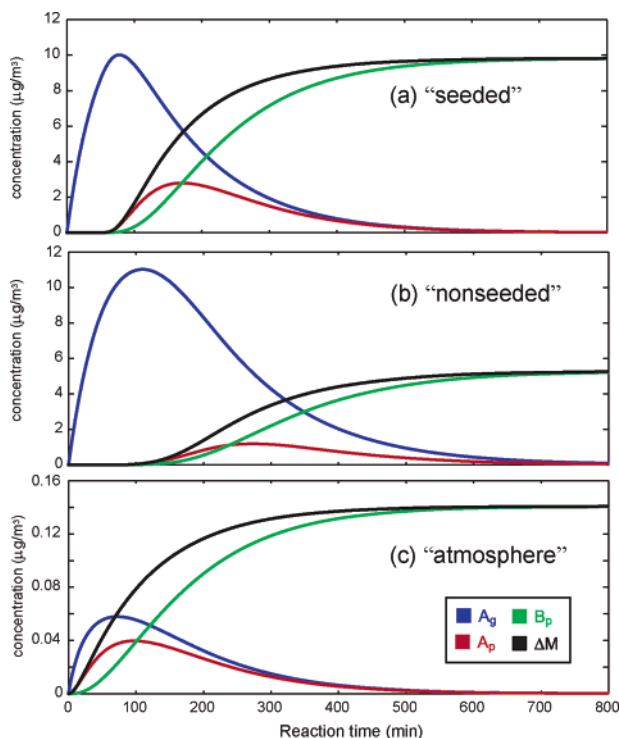
FIGURE 3. Predictions from the mechanism in Figure 2d, showing the time-dependent mass concentrations of key species. In all cases $\alpha = 0.2$, $K_p = 0.1$ m^3 μg^{-1}, $k_{HC} = k_p = 0.015$ min^{-1}, and $k_g = 0.0045$ min^{-1}. (a) Initial concentrations typical of chamber conditions: HC-(0) = 92 μg/m^3, M(0) = 0.1 ng/m^3, and 20 μg/m^3 ammonium sulfate seed. (b) Same as a but with no ammonium sulfate present. (c) Initial concentrations more typical of atmospheric conditions: HC-(0) = 1 μg/m^3 and M(0) = 10 μg/m^3.
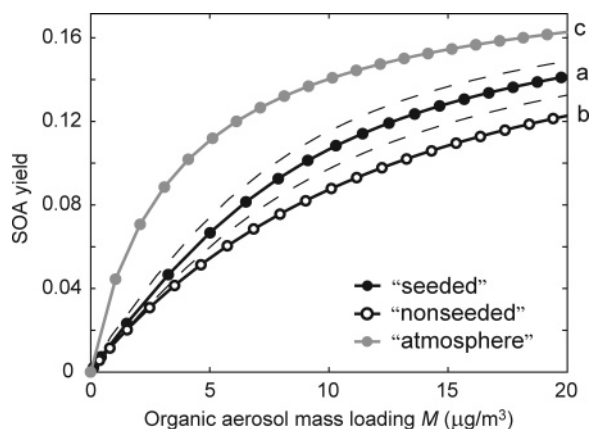
FIGURE 4. Yield curves predicted from the kinetic model. Curves a and b: "seeded" and "nonseeded" cases, in which model parameters are the same as those in Figure 3a and b. M is varied by changing HC(0), as is typically done in chamber studies (increments of 5 μg/m^3). Dashed lines are the same as curve a but with k_p increased by 50% (upper curve) or k_g increased by 25% (lower curve). Curve c: "atmosphere" case, as in Figure 3c. M is varied by changes to M(0) (in increments of 1 μg/m^3); HC(0) is held at 1 μg/m^3.

consistent with the simple partitioning of a single semivolatile compound (Figure 2a). Thus SOA growth is governed by semivolatile partitioning, even though nonvolatile species are also formed. This yield curve (and the others in Figure 4) may be fit to the single-product partitioning expression (eq 1), to obtain effective partitioning parameters; however, these do not match those used in the model, as SOA growth is also strongly influenced by reaction rates (k_{HC}, k_p and k_g).

The effects on SOA yields of the values of these reaction rates are illustrated by the dashed curves in Figure 4. The upper curve is the case in which k_p, the particle-phase reaction rate constant, is increased by 50%; this is consistent with laboratory measurements of enhanced SOA yields in the presence of acidic seed particles, presumably by acid-catalyzed reactions (19, 21, 23, 28). The lower curve shows the effect of increasing k_g, the rate constant for reaction in the gas phase, by 25%, leading to decreased aerosol yields. This is consistent with laboratory evidence that photolysis of semivolatile compounds leads to the formation of relatively volatile products (29−31). In the case where such gas-phase reactions dominate ($k_g > k_p$) and the condensable product is reasonably nonvolatile (high K_p), SOA mass can actually decrease via this volatilization mechanism; such behavior has been observed recently in SOA formation from isoprene oxidation under NO$_x$-free conditions (11). These gas-phase reactions reduce SOA growth by reducing the concentration of the semivolatile species in the gas phase; similarly, an increase in the rate of formation of the semivolatile species, which increases its gas-phase concentration, will increase the SOA yield. The role of hydrocarbon oxidation rate on SOA formation from aromatic photooxidation is discussed in a separate study (15).

Shown in Figure 3b is the reaction profile for the "nonseeded" case, with conditions the same as those in Figure 3a, only without any ammonium sulfate seed present. Nucleation dynamics are not explicitly included in this model, as very small particles (D_p < 5 nm), composed of the trace preexisting organic mass (0.1 ng/m^3), are assumed to be present. The hydrocarbon oxidation (and hence formation of the semivolatile species) is the same as in the "seeded" case, but because of the much lower particle surface area, there is a mass transfer limitation to gas−particle partitioning. Thus A accumulates in the gas phase, even exceeding its saturation vapor pressure, and partitioning (SOA formation) does not occur until later in the reaction. Such an increase in induction period was predicted by Bowman et al. (34), but in that work the semivolatile organic underwent partitioning only (as in Figure 2a), so only the rate of SOA growth was affected. However, in the present case, the reaction A$_g$ → X competes with partitioning, so that longer induction periods lead to more depletion of the semivolatile compound, and less SOA is formed.

As shown in Figure 4 (curve b), yields in the nonseeded case are consistently lower than those in the seeded case, over a range of values of M. Thus this mechanism is qualitatively consistent with the seed effect observed in aromatic photooxidation (Figure 1). Fitting the SOA growth data to this kinetic model is beyond the scope of this work, but simple comparisons are possible; for example, the fact that in the seeded case no induction period is observed even though one is predicted suggests that aromatic oxidation products are less volatile (higher K_p) than simulated in the model. The modeled differences between the seeded and nonseeded cases in Figure 4 are relatively modest, but would be larger under conditions of greater aerosol formation (higher K_p, higher k_p, etc.), or a longer induction period (higher saturation ratio S prior to aerosol growth).

Therefore reactions of semivolatile compounds may have a large influence on SOA yields, and their importance is governed in part by the timing of the onset of gas−particle partitioning. In the seeded case (Figure 3a) this induction period is a result of the initial lack of organic aerosol mass into which the semivolatile organics may partition; in the unseeded case (Figure 3b) it is longer due to the mass-transfer limitation arising from the initially small aerosol surface area. However, in the atmosphere, organic aerosol is generally present, so such effects are not expected. Shown in Figure 3c is a simulation using more realistic tropospheric condi-

tions: a small amount of hydrocarbon ($HC(0) = 1 \ \mu g/m^3$) reacted in the presence of background organic aerosol ($M(0) = 10 \ \mu g/m^3$). These initial conditions are different from those of chamber experiments (Figure 3a and b), in which large amounts of hydrocarbon are reacted with no organic aerosol present; however all other parameters are left unchanged. Because absorbing aerosol is already present, there is no induction period and gas−particle partitioning of the semivolatile species begins immediately. As a result, a smaller fraction of A reacts to form X in the early stages of the reaction. Final aerosol growth (ΔM) is 0.14 $\mu g/m^3$, for an SOA yield of 14% at an organic mass loading of 10.1 $\mu g/m^3$; this yield is significantly higher than that of the "seeded" case (Figure 3a) at nearly the same value of M.

Aerosol yields over a range of organic aerosol loadings are shown in Figure 4, curve c. Unlike for chamber studies (curves a and b), M is varied by changing not $HC(0)$ (which is fixed at $1 \ \mu g/m^3$) but instead the preexisting organic aerosol loading $M(0)$. Over the range of M's shown, SOA yields in the atmospheric case are significantly higher than those in the chamber case, owing to differences in initial partitioning conditions. Such differences in yields are significant (at $M = 5 \ \mu g/m^3$, yield in the "atmosphere" case is about twice that in the "unseeded" case), and are comparable to those from changing reaction conditions (dashed curves).

Implications. We have presented experimental data showing that SOA yields from the photooxidation of aromatic hydrocarbons are enhanced when ammonium sulfate is present. Such an effect is inconsistent with a mechanism of SOA formation that involves only the formation and partitioning of semivolatile species (Figure 2a). Instead, there must be additional processes (chemical reactions and/or surface losses) that affect the concentrations of semivolatile organics; the effect on SOA yields of such reactions, particularly those occurring in the gas phase, have so far received little attention. We propose as a model system the mechanism shown in Figure 2d, in which a semivolatile species may undergo reactions in both the gas phase (reducing its concentration and hence reducing SOA formation) and the particle phase (promoting SOA formation). The seed effect arises from loss of the semivolatile compound during the induction period, which is longer in the nonseeded experiment as a result of mass-transfer limitations. The additional reactions of semivolatile species may also account for a number of other recent experimental observations, such as nonvolatile species in SOA, increased SOA yields with acidic seed, and photochemical loss of SOA mass. An important implication of these reactions is that SOA yields may be quite dependent on detailed reaction conditions. In particular, in laboratory studies of SOA formation, an induction period prior to gas−particle partitioning, during which time gas-phase semivolatile species may be depleted by chemical reaction or wall loss, may lead to lower SOA formation than occurs under atmospheric conditions. Such an effect may contribute to the discrepancies between modeled and measured SOA in the atmosphere (2−4).

Our results suggest that chamber experiments need to be carried out as much as possible under atmospherically realistic conditions, in terms of not only chemistry (oxidant levels, NO_x levels, etc.) but also partitioning (preexisting aerosol). The aromatic photooxidation results presented here indicate that the presence of inorganic seed aerosol can be important for initiating gas−particle partitioning, as lack of aerosol surface area may inhibit uptake of organics; our modeling results suggest the presence of organic aerosol, which allows for immediate absorptive partitioning of organics, may be important as well. Running experiments under conditions similar to those of Figure 3c is infeasible, but the presence of even a small amount of organic seed aerosol (a few $\mu g/m^3$) would eliminate the induction period,

substantially reducing differences between "chamber" and "atmospheric" conditions. The loading of preexisting organic seed is a parameter that has not been explored in chamber experiments of SOA formation thus far, and certainly warrants future study.

The effect of preexisting organic aerosol is expected to be most important for reactions that form semivolatile compounds with relatively high vapor pressures (low K_p's), and hence which exhibit significant induction times. For reactions involving relatively low-volatility condensable compounds (high K_p's), SOA growth begins very early in the reaction. For these reactions, such as α-pinene ozonolysis (36, 37), the induction period is negligible, and gas−particle partitioning occurs throughout the experiment at atmospherically relevant levels.

The induction periods described here are a result of the buildup of semivolatile products in the gas-phase prior to gas−particle partitioning; induction periods may arise from other effects as well. Examples include photooxidation reactions carried out under high-NO_x conditions, in which SOA formation does not begin until [NO] falls to ppb levels (e.g., 11, 14), and reactions involving multiple rate-limiting steps to SOA formation (34, 36). In both cases the delay is in the formation of the semivolatile species rather than in gas−particle partitioning, so may occur under atmospheric conditions. The sources of (and relationships between) different induction periods need to be understood in order for chamber yield measurements to accurately represent atmospheric conditions.

We emphasize that the mechanism shown in Figure 2d, while likely to be valid for some semivolatile organics, is not intended as a general scheme describing the chemistry of all condensable compounds. Most SOA-forming reactions involve a large number of semivolatiles, which may react via any number of mechanisms, including those shown in Figure 2. This mechanism is instead used as a model system illustrating the potential influence of reactions of semivolatile species on SOA formation, and the resulting dependence of SOA yields on reaction and partitioning conditions. Such reactions are often not treated explicitly in models of SOA formation, but certainly occur for a wide range of compounds: most organics are susceptible to reaction with OH, and loss to chamber walls is a potential sink for species that are efficiently taken up to the aerosol phase. If these processes are fast on the time scale of chamber experiments, they may have a substantial impact on SOA growth, and on the relationship between chamber studies and real atmospheric conditions. Only by explicitly including such reactions in models of SOA formation, or by making SOA yield measurements under oxidative and partitioning conditions relevant to the atmosphere, can such effects be taken fully into account.

Acknowledgments

Literature Cited

(1) Kanakidou, M.; Seinfeld, J. H., Pandis, S. N.; Barnes, I.; Dentener, F. J.; Facchini, M. C.; Van Dingenen, R.; Ervens, B.; Nenes, A.; Nielsen, C. J. Organic aerosol and global climate modelling: a review. *Atmos. Chem. Phys.* **2005**, *5*, 1053−1123.

(2) De Gouw, J. A.; Middlebrook, A. M.; Warneke, C.; Goldan, P. D.; Kuster, W. C.; Roberts, J. M.; Fehsenfeld, F. C.; Worsnop, D. R.; Canagaratna, M. R.; Pszenny, A. A. P. Budget of organic carbon in a polluted atmosphere: Results from the New England Air Quality Study in 2002. *J. Geophys. Res.* **2005**, *110*, D16305, doi: 10.1029/2004JD005623.

(3) Heald, C. L.; Jacob, D. J.; Park, R. J.; Russell, L. M.; Huebert, B. J.; Seinfeld, J. H.; Liao, H.; Weber, R. J. A large organic aerosol source in the free troposphere missing from current models. *Geophys. Res. Lett.* **2005**, *32*, L18809, doi:10.1029/2005GL023831.

(4) Volkamer R.; Jimenez, J. L.; San Martini, F.; Szepina, K.; Zhang, Q.; Salcedo, D.; Molina, L. T.; Worsnop, D. R.; Molina, M. J. Secondary organic aerosol formation from anthropogenic air pollution: rapid and higher than expected. *Geophys. Res. Lett.* **2006**, *33*, L17811, doi:10.1029/206GL026899.

(5) Pankow, J. F. An absorption model of gas/particle partitioning of organic compounds in the atmosphere. *Atmos. Environ.* **1994**, *28A*, 185−188.

(6) Pankow, J. F. An absorption model of the gas/aerosol partitioning involved in the formation of secondary organic aerosol. *Atmos. Environ.* **1994**, *28A*, 189−193.

(7) Odum J. R.; Hoffmann, T.; Bowman, F.; Collins, D.; Flagan, R. C.; Seinfeld, J. H. Gas/particle partitioning and secondary organic aerosol yields. *Environ. Sci. Technol.* **1996**, 3*0*, 2580−2585.

(8) Seinfeld, J. H.; Pankow, J. F. Organic atmospheric particulate material. *Annu. Rev. Phys. Chem.* **2003**, *54*, 121−140.

(9) Cocker, D. R., III; Flagan, R. C.; Seinfeld, J. H. State-of-the-art chamber facility for studying atmospheric aerosol chemistry. *Environ. Sci. Technol.* **2001**, *35*, 2594−2601.

(10) Keywood, M. D.; Varutbangkul, V.; Bahreini, R.; Flagan, R. C.; Seinfeld, J. H. Secondary organic aerosol formation from the ozonolysis of cycloalkenes and related compounds. *Environ. Sci. Technol.* **2004**, *38*, 4157−4164.

(11) Kroll, J. H.; Ng, N. L.; Murphy, S. M.; Flagan, R. C.; Seinfeld, J. H. Secondary organic aerosol formation from isoprene photooxidation. *Environ. Sci. Technol.* **2006**, *40*, 1869−1877.

(12) Odum, J. R.; Jungkamp, T. P. W.; Griffin, R. J.; Forstner, H. J. L.; Flagan, R. C.; Seinfeld, J. H. Aromatics, reformulated gasoline, and atmospheric organic aerosol formation. *Environ. Sci. Technol.* **1997**, *31*, 1890−1897.

(13) Song, C.; Na, K. Cocker, D. R., III. Impact of the hydrocarbon to NO$_x$ ratio on secondary organic aerosol formation. *Environ. Sci. Technol.* **2005**, *39*, 3143−3149.

(14) Johnson, D.; Jenkin, M. E.; Wirtz, K.; Martín-Reviejo, M. Simulating the formation of secondary organic aerosol from the photooxidation of toluene. *Environ. Chem.* **2004**, *1*, 150−165.

(15) Ng, N. L.; Kroll, J. H.; Chan, A. W. H.; Chhabra, P.; Flagan, R. C.; Seinfeld, J. H. Secondary organic aerosol formation from m-xylene, toluene, and benzene. *Atmos. Chem. Phys. Discus.,* **2007**, *7*, 4085−4126.

(16) Cocker, D. R., III; Mader B. T.; Kalberer, M.; Flagan, R. C.; Seinfeld, J. H. The effect of water on gas−particle partitioning of secondary organic aerosol: II. *m*-xylene and 1,3,5-trimethylbenzene photooxidation systems. *Atmos. Environ.* **2001**, *35*, 6073−6085.

(17) Kroll, J. H.; Seinfeld, J. H. Representation of secondary organic aerosol (SOA) laboratory chamber data or the interpretation of mechanisms of particle growth. *Environ. Sci. Technol.* **2005**, *39*, 4159−4165.

(18) Tobias, H. J.; Ziemann, P. J. Thermal desorption mass spectrometric analysis of organic aerosol formed from reactions of 1-tetradecene and O$_3$ in the presence of alcohols and carboxylic acids. *Environ. Sci. Technol.* **2000**, *34*, 2105−2115.

(19) Tolocka, M. P.; Jang, M.; Ginter, J. M.; Cox, F. J.; Kamens, R. M.; Johnston, M. V. Formation of oligomers in secondary organic aerosol. *Environ. Sci. Technol.* **2004**, *38*, 1428−1434.

(20) Kalberer, M.; Paulsen, D.; Sax, M.; Steinbacher, M.; Dommen, J.; Prevot, A. S. H.; Fisseha, R.; Weingartner, E.; Frankevich, V.; Zenobi, R.; Baltensperger, U. Identification of polymers as major components of atmospheric organic aerosols. *Science* **2004**, *303*, 1659−1662.

(21) Iinuma, Y.; Böge, O.; Gnauk, T.; Herrmann, H. Aerosol-chamber study of the α-pinene/O$_3$ reaction: influence of particle acidity on aerosol yields and products. *Atmos. Environ.* **2004**, *38*, 761−773.

(22) Gao, S.; Ng, N. L.; Keywood, M.; Varutbangkul, V.; Bahreine, R.; Nenes, A.; He, J.; Yoo, K. Y.; Beauchamp, J. L.; Hodyss, R. P.; Flagan, R. C.; Seinfeld, J. H. Particle phase acidity and oligomer formation in secondary organic aerosol. *Environ. Sci. Technol.* **2004**, *38*, 6582−6589.

(23) Gao, S.; Keywood, M.; Ng, N. L.; Suratt, J.; Varutbangkul, V.; Bahreini, R.; Flagan, R. C.; Seinfeld, J. H. Low-molecular weight and oligomeric components in secondary organic aerosol from the ozonolysis of cycloalkenes and α-pinene. *J. Phys. Chem. A* **2004**, *108*, 10147−10164.

(24) Surratt, J. D.; Murphy, S. M.; Kroll, J. H.; Ng, N. L.; Hildebrandt, L.; Soroooshian, A.; Szmigielski, R.; Vermeylen, R.; Maenhaut, W.; Claeys, M.; Flagan, R. C.; Seinfeld, J. H. Chemical composition of secondary organic aerosol formed in the photooxidation of isoprene. *J. Phys. Chem. A* **2006**, *110*, 9665−9690.

(25) Liggio, J.; Li, S.-M.; McLaren, R. Heterogeneous reactions of glyoxal on particulate matter: Identification of acetals and sulfate esters. *Environ. Sci. Technol.* **2005**, *39*, 1532−1541.

(26) Liggio, J.; Li, S.-M. Organosulfate formation during the uptake of pinonaldehyde on acidic sulfate aerosols. *Geophys. Res. Lett.* **2006**, *33*, L13808, doi:10.1029/2006GL026079.

(27) Surratt, J. D.; Kroll, J. H.; Kleindienst, T. E.; Edney, E. O.; Claeys, M.; Soroooshian, A.; Ng, N. L; Offenberg, J. H.; Lewandowski, M.; Jaoui, M.; Flagan, R. C.; Seinfeld, J. H. Evidence for organosulfates in secondary organic aerosol. *Environ. Sci. Technol.* **2007**, *41* (2), 517−527.

(28) Jang, M.; Czoschke, N. M.; Lee, S.; Kamens, R. M. Heterogeneous atmospheric aerosol production by acid-catalyzed particle-phase reactions. *Science* **2002**, *298*, 814−817.

(29) Presto, A. A.; Huff Hartz, K. E.; Donahue, N. M. Secondary organic aerosol production from terpene ozonolysis. 1. Effect of UV radiation. *Environ. Sci. Technol.* **2005**, *39*, 7036−7045.

(30) Gomez, A. L.; Park, J.; Walser, M. L.; Lin, A.; Nizkorodov, S. A. UV photodissociation spectroscopy of oxidized undecylenic acid films. *J. Phys. Chem. A* **2006**, *110*, 3854−3592.

(31) Park, J.; Gomez, A. L.; Walser, M. L.; Lin, A.; Nizkorodov, S. A. Ozonolysis and photolysis of alkene-terminated self-assembled monolayers on quartz nanoparticles: implications for photochemical aging of organic aerosol particles. *Phys. Chem. Chem. Phys.* **2006**, *8*, 2506−2512.

(32) Hastings, W. P.; Koehler, C. A.; Bailey, E. L.; De Haan, D. O. Secondary organic aerosol formation by glyoxal hydration and oligomer formation: Humidity effects and equilibrium shifts during analysis. *Environ. Sci. Technol.* **2005**, *39*, 8728−8735.

(33) Kroll, J. H.; Ng, N. L.; Murphy, S. M.; Varutbangkul, V.; Flagan, R. C.; Seinfeld, J. H. Chamber studies of secondary organic aerosol growth by reactive uptake of simple carbonyl compounds, *J. Geophys. Res.* **2005**, *110*, D23207, doi:10.1029/2005JD006004.

(34) Bowman, F. M.; Odum, J. R.; Seinfeld, J. H.; Pandis, S. N. Mathematical model for gas-particle partitioning of secondary organic aerosols. *Atmos. Environ.* **1997**, *31*, 3921−3931.

(35) Schweitzer, F.; Magi, L.; Mirabel, P.; George, C. Uptake rate measurements of methanesulfonic acid and glyoxal by aqueous droplets. *J. Phys. Chem. A* **1998**, *102*, 593−600.

(36) Ng, N. L.; Kroll, J. H.; Keywood, M. D.,; Bahreinei, R.; Varatbangkul, V.; Flagan, R. C.; Seinfeld, J. H.; Lee, A.; Goldstein, A. H. Contribution of first- versus second-generation prducts to secondary organic aerosols formed in the oxidation of biogenic hydrocarbons. *Environ. Sci. Technol.* **2006**, *40*, 2283−2297.

(37) Presto, A. A.; Donahue, N. M. Investigation of α-pinene + ozone secondary organic aerosol formation at low total aerosol mass. *Environ. Sci. Technol.* **2006**, *40*, 3536−3543.